Weierstraß-Institut
für Angewandte Analysis und Stochastik

Leibniz-Institut im Forschungsverbund Berlin e. V.

Preprint ISSN 2198-5855

Nonlinear dynamical properties of frequency swept fiber-based semiconductor lasers

Svetlana Slepneva[1,2,3], Alexander Pimenov[4]

submitted: April 28, 2021

[1] Université Côte d'Azur
CNRS
INPHYNI
Parc Valrose
06108 Nice
France
E-Mail: svetlana.slepneva@gmail.com

[2] Centre for Advanced Photonics and Process Analysis and
Department of Physical Sciences
Cork Institute of Technology
Cork
Ireland

[3] Tyndall National Institute
University College Cork
Lee Maltings
Dyke Parade
Cork
Ireland

[4] Weierstrass Institute
Mohrenstr. 39
10117 Berlin
Germany
E-Mail: alexander.pimenov@wias-berlin.de

No. 2839
Berlin 2021

2010 *Physics and Astronomy Classification Scheme.* 42.55.Px, 42.65.Sf, 42.60.Mi, 42.55.Ah, 02.30.Ks.

Key words and phrases. Semiconductor lasers, swept source, nonlinear dynamics, turbulence, dispersion.

SS would like to acknowledge Marie Sklodowska-Curie Individual Fellowships European H2020-MSCA-IF-2017, ICOFAS project (800290). AP acknowledges the support of the joint DFG-RSF Project 445430311. The authors would like to acknowledge valuable support from G. Huyet, A. G. Vladimirov, S. P. Hegarty, B. Kelleher, M. Giudici, S. Amiranashvili.

Edited by
Weierstraß-Institut für Angewandte Analysis und Stochastik (WIAS)
Leibniz-Institut im Forschungsverbund Berlin e. V.
Mohrenstraße 39
10117 Berlin
Germany

Fax: +49 30 20372-303
E-Mail: preprint@wias-berlin.de
World Wide Web: http://www.wias-berlin.de/

Nonlinear dynamical properties of frequency swept fiber-based semiconductor lasers

Svetlana Slepneva, Alexander Pimenov

Abstract

We investigate dynamics of semiconductor lasers with fiber-based unidirectional ring cavity that can be used as frequency swept sources. We identify key factors behind the reach dynamical behaviour of such lasers using state-of-the-art experimental and analytical methods. Experimentally, we study the laser in static, quasi-static and synchronisation regimes. We apply experimental methods such as optical heterodyne or electric field reconstruction in order to characterise these regimes or study the mechanisms of transition between them. Using a delay differential equation model, we demonstrate that the presence of chromatic dispersion can lead to destabilisation of the laser modes through modulational instability, which results in undesirable chaotic emission. We characterise the instability threshold both theoretically and experimentally, and demonstrate deterioration of the FDML regime near the threshold.

1 Introduction

The interest to swept source lasers is mostly driven by variety of their applications, especially in such actively developing areas as Optical Coherence Tomography imaging [1, 2] and LiDARs [3]. Swept source lasers generate coherent radiation that sweeps over a broad optical bandwidth in infrared range at high speed. In some applications the use of an optical sweep eliminates the need for mechanical scanning thus increasing the speed and quality of imaging. The tuning bandwidth can exceed 100 nm and the sweep rate reaches 5 MHz [4] with a narrow instantaneous linewidth on the order of MHz [5]. While the leading swept source technologies in the market are based on semiconductor gain medium, the mechanisms of sweep generation are different [6]. In order to meet requirements of a particular application, one can choose between swept sources with a single mode tuning, such as in Micro-electro-mechanical system-based (MEMS) tunable Vertical Cavity Surface Emitting Lasers (VCSEL) [5], or pulsed output, which can be achieved using different approaches [7, 8, 9], or get advantage of all-electrically controlled sweep, such as in akinetic multi-section swept source lasers [10]. Understanding the physics of sweep generation is important to overcome current limitations and broaden the area of applications of swept source lasers.

Here, we present the study on the dynamical regimes of a swept source laser based on long ring fiber including a semiconductor optical amplifier (SOA) as a gain medium and a Fabry-Pérot tunable filter whose transmission is periodically modulated. The fastest tuning speed and a narrow linewidth of a long cavity laser can be achieved when the filter transmission is modulated in resonance with the cavity roundtrip time, which is implemented by introducing a long single mode fiber delay into the cavity. This regime is known as Fourier domain mode locking (FDML) [11]. The pioneering characteristics of FDML lasers were possible to attain by introducing precise dispersion compensation [12] or buffering [13]. Furthermore, the laser configuration can be modified to generate pulsed output in infrared [8] or visible [9] range.

DOI 10.20347/WIAS.PREPRINT.2839 Berlin 2021

Recently, active application driven development of long cavity lasers has inspired a new perspective of research on such devices, particularly, in the field of nonlinear dynamics. A typical FDML laser can have a cavity length of tens of km and intra-cavity bandpass filter of several gigahertz, therefore such laser can simultaneously generate huge amount of modes making them excellent test beds to study nonlinear effects in complex systems. Such lasers have recently demonstrated their ability to operate in various dynamical regimes under controlled parameters [14, 15, 16, 17, 18, 19, 20, 21]. Long ring cavity semiconductor lasers can emit stable or turbulent radiation [14, 22] and can be used to study the transition to turbulence in analogy with hydrodynamical systems [23]. Recent studies have shown that unstable localised structures mediate the transition from stable to turbulent regimes in the case of normal dispersion [15], while only turbulent regime occurs in anomalous dispersion [22]. Understanding nonlinear properties of long fiber cavity lasers with a semiconductor gain medium provides background for a number of potential applications, such as optical reservoir computing [24], photonics information processing [25] and optical networks for studying complex systems [26].

Different theoretical models were developed to describe semiconductor long cavity lasers [17, 18, 27]. Remarkably, a simple system of two delay differential equations (DDEs) can capture the full variety of nonlinear dynamical regimes of short [28] and long cavity swept sources [14, 16] in the case of normal dispersion, whereas anomalous dispersion of a long fiber delay line can be accurately accounted for using an additional distributed delay term [22]. Stability analysis of the constant wave (CW) regimes of a static laser (lasing modes) in the limit of large delay can help to explain appearance of the turbulence during sweeping as the result of modulational instability (MI) of CW regimes. Since turbulence in anomalous dispersion is caused by a MI of all the laser modes, this distributed term can be theoretically replaced by a single ordinary differential equation preserving the same effect [19]. We perform numerical simulations of an FDML laser in quasi-static regime under the influence of noise using the DDE model and discuss the effect of MI on the quality of the laser output in direct comparison with the experimental data.

2 Experimental characterisation of long cavity swept source laser

2.1 The laser

The configuration of the laser is shown in Fig. 1. The laser consisted of a single mode fiber-based ring cavity that included an SOA as a gain medium with 88.1 nm optical 3 dB bandwidth, 32.1 dB small signal gain, and a narrow transmission bandwidth (8 GHz) tunable Fabry-Pérot filter. The filter transmission was modulated by a signal generator. Several optical isolators in the cavity ensured unidirectional light propagation. A part of the light from the cavity was tapped out using $50{:}50$ coupler. The total length of the basic cavity was composed of the total length of all the fiber pigtails of all the components, corresponding to about 30 m. The polarisation was controlled with polarisaton paddles. The length of the cavity could be varied by including additional single mode fiber (SMF-28). The measured loss of 20 km of fiber (required for FDML regime) was 8.94 dB. The manufacturer specified the zero dispersion wavelength within the range of 1302-1322 nm.

2.2 Characterisation techniques

The temporal evolution of the laser intensity was measured by coupling the laser output to a fast detector and fast real time oscilloscope with the 12 GHz matching bandwidth. The intra-sweep optical

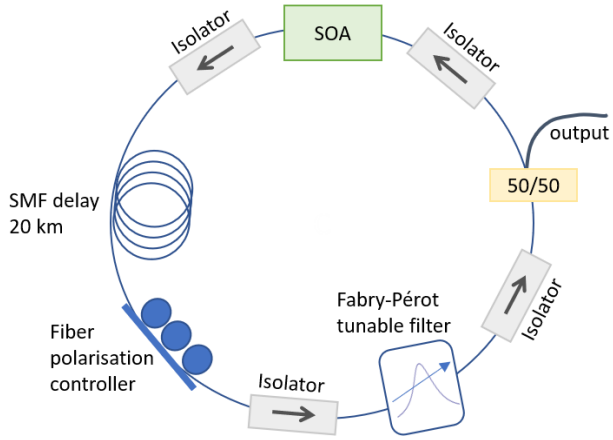

Figure 1: Experimental setup of a long cavity semiconductor laser.

properties were measured using the optical heterodyne technique. The output of the swept source was mixed in a fiber coupler with a single mode tunable laser source (TLS) of a narrow (100 kHz) linewidth, which served as a local oscillator. The beating signal was observed over the part of the sweep corresponding to the detection bandwidth, and by varying the output wavelength of the TLS, the entire sweep was scanned. Despite of the simplicity of such technique, it is a useful tool to provide the reference measurement of the intra-sweep evolution of the optical frequency and estimate the linewidth [28, 29].

For the full characterisation of light emitted by a laser, both the amplitude and phase of the electric field needed to be measured. For example, in order to characterise a mode locked laser, the electric field can be reconstructed using techniques such as frequency resolved optical gating (FROG) [30]. However, this and similar techniques could not be applied to swept source lasers, as they allowed for measuring the average pulse intensity and phase profile, and it was demonstrated that such approach was not suitable for reconstruction of aperiodic dynamics similar to that observed in quantum dot mode-locked lasers when they emit aperiodic pulses above threshold [31]. In order to study swept source lasers we used another technique which provided access to the complex electric field along a single sweep [32]. This technique has proven to be a useful tool for characterisation of different swept source lasers [29, 32], in particular, access to the full electric field allowed calculation of such properties as coherence time, instantaneous linewidth, instantaneous spectra, as well as demonstrate the modal interaction [33]. In addition, key performance parameters important for applications such as coherence roll-off and point spread function can also be obtained from this measurement by numerical simulation of Mach-Zehnder interferometer [32]. The technique was based on mixing an output sweep with the delayed version of itself in a fiber coupler with three identical inputs and outputs (a 3x3 coupler) [34]. The difference between the phase $\phi(t)$ and the delayed phase $\phi(t-\tau)$ was calculated from the intensity time traces recorded at the three outputs of the coupler [35], and then, temporal evolution of the phase was retrieved following [36]. Simultaneous reading of the laser intensity allowed for the reconstruction of the electric field. When the sweep was narrow enough or when the laser operated at a fixed wavelength, the TLS was used as a reference laser at one of the inputs of the 3x3 coupler to obtain the phase of the laser in the frame of the reference laser. This approach was initially applied to characterise excitable pulses in lasers with external optical injection [35]. In the context of swept source lasers, it was used for characterisation of localised structures emitted by a long laser [15, 16].

2.3 Experimental results and discussion

We analysed the dynamics of the long cavity laser operating in three regimes: a static regime when the filter transmission was fixed and the output frequency was constant, a quasistatic tuning when the filter transmission was slowly modulated, and the regime of synchronisation (FDML).

First, the filter transmission was fixed in normal dispersion region at 1290 nm. The variable parameter was the bias current of the SOA. At the bias current just above its threshold value, the laser emitted multiple drops per roundtrip and the number of drops reduced with increase of the bias current. These drops demonstrated turbulent structure and at the fixed parameters, they remained stable for many roundtrips. Recently, the stability of the drops was investigated using the electric field reconstruction technique [16]. The analysis of the reconstructed optical frequency revealed that the drops remained outside of the filter resonance, therefore, as they circulated in the cavity and amplified by the SOA, they still experienced non-compensated losses, which explained their long term stability. Such structures known as Nozaki-Bekki holes were previously theoretically predicted as solution to complex Ginzburg–Landau equation and have not been previously demonstrated in an optical system [37, 38]. At higher bias current values (about 2.5 times the laser threshold current value) the laser operated in CW regime with no drops (Fig. 2 (a)). At the fixed parameters, the laser remained stable, but a slight blue shift of the filter frequency, which could be induced either manually or due to noise, destabilised the CW regime and the laser behaved chaotically (Fig. 2 (b)). The laser was re-stabilised by the red shifting of the filter transmission. In addition, at the same parameters, a random switching between these two regimes was observed (Fig. 2 (c)).

When the filter transmission was set to longer wavelength (1345 nm) in order to achieve lasing in anomalous dispersion regime, the laser output remained always chaotic (Fig. 2 (d) and (e)). No stable lasing was achieved after the filter passed the zero dispersion point disregarding the bias current, however, the transition wavelength varied as a function of the cavity length indicating the influence of dispersion [22]. The measured threshold wavelength as a function of the length of the fiber at which the transition from bi-stable to chaotic dynamic occurred is shown in (Fig. 2 (f)). Such an observation indicated that the dispersion of the optical fiber played an important role in the stability of the laser output as it led to a wavelength dependent roundtrip time as shown in Fig. 2 (g).

In a quasistatic regime, the filter was slowly modulated at a few hundreds of mHz. In a normal dispersion regime, when the filter transmission wavelength was constantly increasing (forward sweep), the laser emitted a sequence of jumps form one stable output to another with power dropouts in between (Fig. 3 (a)). By applying an optical heterodyne technique, it was shown that each stable region was associated with a single mode emission of the laser. The frequency difference between the consecutive steady-state solutions was $\sim$4 GHz. This value was several orders of magnitude larger than the cavity mode spacing, but of the same order of magnitude as the filter bandwidth. This indicated that as the filter was moving out of resonance, the lasing mode was loosing its stability and occasionally jumped to another stable mode close to the maximum gain of the filter. The increase of the modulation frequency of the filter leads to the gradual decrease of the duration of the stable regions between the transients until the stable regions disappeared (Fig. 3 (b)). Similar behaviour was observed in short cavity MEMS laser at slow sweeping rates [28, 39]. For the decreasing filter transmission wavelength (backward sweep), the laser demonstrated chaotic emission and the Fourier transform of the beating signal showed the instantaneous linewidth on the order of 5 GHz which corresponded to the filter bandwidth. This asymmetry in the laser intensity versus the sweep direction is associated with the SOA nonlinearity [14, 40] and is typically present in other semiconductor swept source lasers.

In anomalous dispersion regime, when the filter was set to scan the wavelengths longer than 1319 nm,

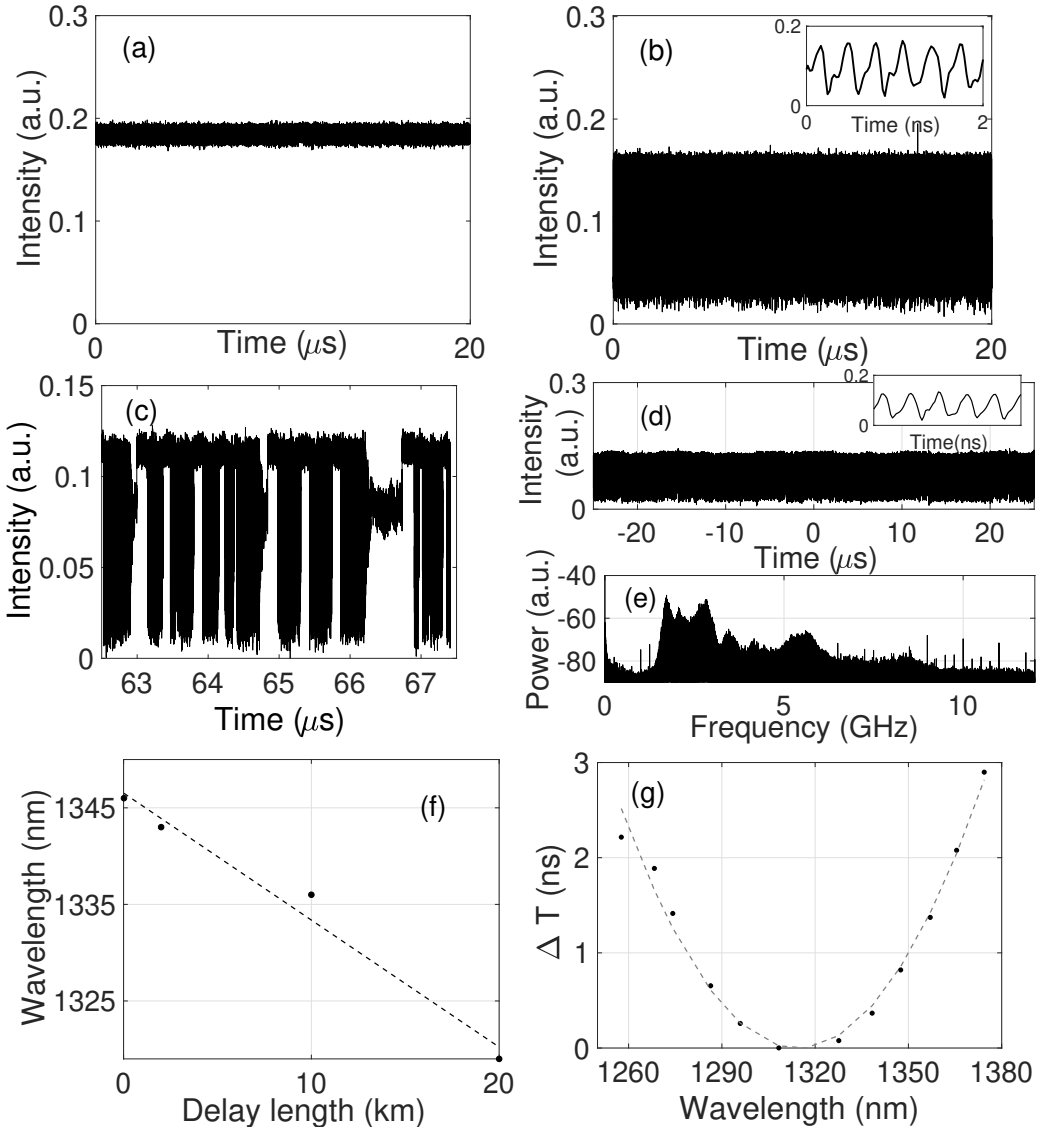

Figure 2: Laser intensity time traces in static regime for the case of normal dispersion demonstrating cw lasing (a), chaotic lasing (b) and random switching between stable and chaotic lasing (c). Intensity time trace (d) and corresponding power spectra measured by electrical spectrum analyser (e) in the case of anomalous dispersion demonstrating chaotic emission. Instability threshold as a function of fiber length (f). The insets in (b) and (d) show zooms of the chaotic signals. (g) shows the measured roundtrip time in the reference of its minimum value as a function of wavelength for 20 km fiber delay (points) and its quadratic fit (solid line).

the laser exhibited chaotic output regardless of the sweep direction (Fig. 3 (c)) and the asymmetry between the forward and backward sweeps only appeared when the filter frequency reached some threshold value (Fig. 3 (d)). At such slightly higher sweeping speeds, the time trace was similar to that observed at shorter wavelengths except that the dynamic did not show any relaxation toward CW solutions.

Next, we considered the laser operating in FDML regime. Ideally, the filter frequency f_{filter} and the frequency corresponding to the roundtrip time of light in the cavity $f_{RT} = \frac{1}{T_{RT}}$ should be equal for all the wavelengths within the sweeping range and the laser emits a frequency modulated output corresponding to single modes in the filter frame [14]. The first FDML lasers were built to sweep around

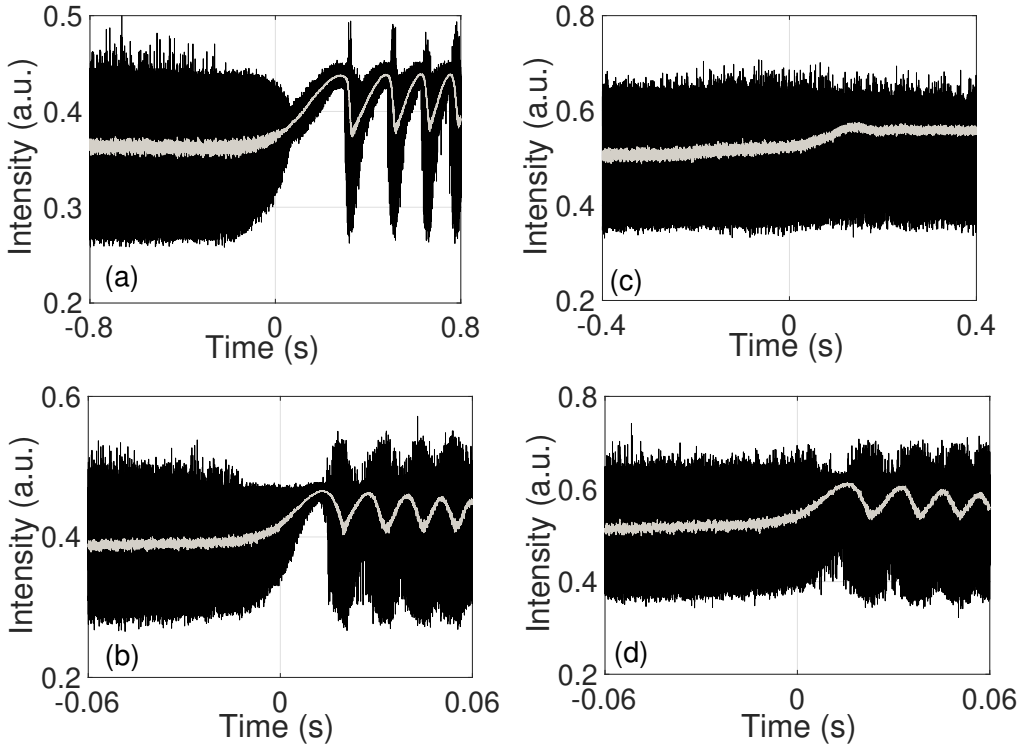

Figure 3: Intensity time traces in quasistatic regime corresponding to the case of normal dispersion and modulation frequencies of 100 mHz (a) and 1600 mHz (b), and anomalous dispersion and modulation frequencies of 200 mHz (c) and 1600 mHz (d). Zero time indicates the change of the sweep direction from backward (negative time) to forward (positive time) sweep direction. Only a part of the full sweep is shown. Numerically filtered traces are shown in grey.

1300 nm in order to decrease the effect of dispersion. Soon, it was demonstrated that it was possible to minimise the effect of dispersion by introducing a dispersion compensated fiber and this significantly improved the performance of FDML, especially, the instantaneous coherence length [41]. However, this approach could only work for either normal or anomalous dispersion regime, limiting the scanning range, and required precise temperature and polarisation control. Broadband dispersion compensation was achieved by introducing a chirped fiber Bragg grating, tailored to compensate simultaneously normal and anomalous dispersion, into the cavity, however, at the cost of complexity of the system [12].

In our experiment, due to the presence of chromatic dispersion, a stable output was only achieved when sweeping a small range of wavelengths below 0.5 nm in normal dispersion regime or around a zero dispersion point and the dynamics of the FDML laser depended on detuning parameter $\delta = f_{filter} - f_{RT}$. At a very small value of δ (on the order of sub-mHz), the stable regime was locally destabilised and the intensity corresponded to the CW output with inserts of turbulent regions. The transition points between CW and turbulent regions was fixed within the sweep. As detuning increased, the sweep demonstrated asymmetry similar to that observed in quasistatic case. In order to study the asymmetry as a function of detuning, the laser was set to sweep a few nm in a normal dispersion regime (Fig. 4 (a)). First, we set the frequency modulation below the resonant frequency of the lowest wavelength, thus $f_{filter} < f_{RT}$ held for all wavelengths and the laser was all-negatively detuned. In this case the backward sweep demonstrated steps between stable regimes and the forward sweep demonstrated chaotic emission (Fig 4 (b-1)). Recently, it has been demonstrated that the transitions between the stable regions in the stepwise regime corresponded to an interesting example of transition between stable and turbulent radiation [15]. The electric field reconstruction technique revealed

that such transition was mediated by formation of unstable localised structures, which were moving towards the main turbulent region and developing into turbulent puffs. When the filter modulation frequency was increased to sweep in resonance with some wavelength within the sweep, one part of the sweep was still negatively detuned while the other part was positively detuned. For the backward sweep, the negatively detuned part still demonstrated steps, while the positively detuned part started to demonstrate chaotic behaviour and for the forward sweep the situation was reversed (Fig 4 (b-2)). As δ was further increased, the asymmetry versus the sweep direction gradually altered (Fig 4 (b-3)) and when the detuning became positive for all wavelengths, the asymmetry was fully reversed (Fig 4 (b-4)). By analysing the laser emission in the frame of the filter, it can be demonstrated that the dynamics of all-positively and all-negatively detuned FDML is equivalent to the quasistatic tuning at a frequency equal to the absolute value of detuning [14].

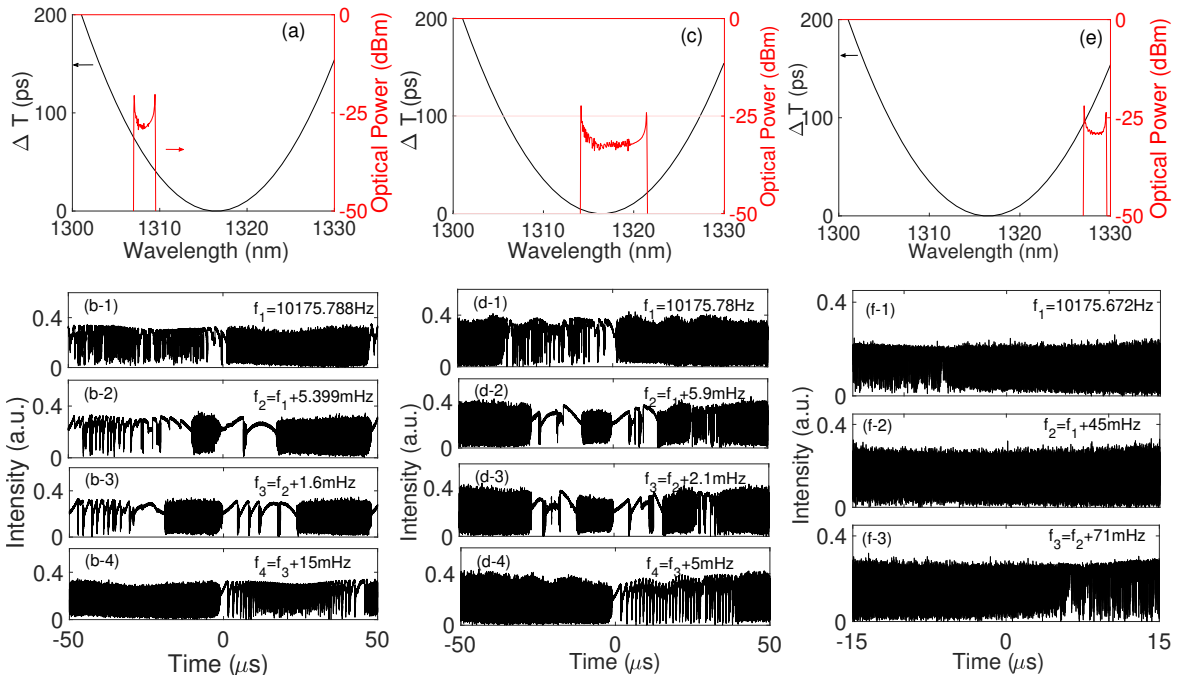

Figure 4: Optical spectra (red) of FDML laser in normal dispersion (a), around zero dispersion (c) and anomalous dispersion (d). Black curve ΔT corresponds to the measured variation of the cavity roundtrip time (see Fig. 1 (b)). The time traces below show the intensity for the increasing values of detuning starting from its lowest value f_1 at the top trace and successively increased by indicated values in normal dispersion (b-1)-(b-4), around zero dispersion (d-1)-(d-4) and anomalous dispersion (f-1)-(f-3) regimes.

An interesting case was observed when the FDML laser was sweeping around the zero dispersion point(Fig. 4 (c)). For the value of detuning δ negative for all the wavelengths, a usual asymmetry within the sweep was observed (Fig. 4 (d-1)) and the asymmetry was reversed for δ positive for all the wavelengths (Fig. 4 (d-4)). However, for intermediate values of detuning, the filter modulation was in resonance not only with one wavelength within the sweep, but with two, thus the forward sweep demonstrated three regimes: chaotic - steps - chaotic, the backward sweep demonstrates three regimes: steps - chaotic - steps, and the transition points between different regimes indicated the location of the resonant wavelengths (Fig. 4 (d-2) and (d-3)).

Finally, the filter was set to sweep in anomalous dispersion regime (Fig. 4 (e)). The CW output was not possible to achieve when the laser operated above the zero dispersion point. The synchronisation with some wavelength within a sweep demonstrated chaotic emission similarity to the static case (Fig. 4 (f-

2)) while in the case of detuning, the asymmetry appeared (Fig. 4 (f-1) and (f-2)) reminiscent of the quasistatic tuning (compare with Fig. 3 (c) and (d)).

These results indicate that the lasing regimes in normal dispersion region and around zero dispersion are similar, but the presence of anomalous dispersion leads to additional instabilities. Hence, in order to describe the laser theoretically, one can neglect the presence of dispersion for the laser operating in normal dispersion regime, however, the dispersion term must be present in the model in order to include the effect of anomalous dispersion.

3 Theoretical model

3.1 DDE model

We consider a delayed model of the laser comprising a short SOA section, linear frequency selective spectral filter, and a long dispersive fiber delay line. This device can be described using a DDE model Ref. [14, 22]

$$\frac{dA}{dt} + (\gamma - iw)A = \gamma\sqrt{\kappa}e^{(1-i\alpha)G/2+i\varphi}B(t-T) + \epsilon\xi(t), \tag{1}$$

$$\frac{dG}{dt} = \gamma_g\left[g_0 - G - (e^G - 1)\left|B(t-T)\right|^2\right], \tag{2}$$

where $A(t)$ and $B(t)$ are the electric field envelopes at the entrance and at the output of the fiber delay line, respectively; $G(t)$ represents saturable gain in the SOA section, and T is the cavity round-trip time. The parameters γ and w describe the spectral filter bandwidth and the central frequency of the filter, $\kappa < 1$ represents linear nonresonant losses in the SOA, α is the linewidth enhancement factor, φ describes the detuning between a reference frequency and the considered cavity mode, γ_g is the the carrier relaxation rate in SOA, and g_0 is the pump parameter. Sweeping can be achieved by changing central frequency of the filter $w = \Delta(t)$ periodically in time. The last term in equation (1) describes spontaneous emission noise using a complex Gaussian white noise term $\xi = \xi_1 + i\xi_2$ with strength ϵ satisfying $\langle\xi_i\rangle = 0$ and $\langle\xi_i(t)\xi_j(t')\rangle = \delta_{i,j}\delta(t-t')$.

For zero dispersion we can account for linear losses in the fiber delay line using the parameter κ and assume $B(t) = A(t)$, thus closing the system (1)-(2) [14]. This model represents well the most important dynamical features of the FDML laser, and can successfully detect various regimes of operation with different patterns of both short-cavity swept sources [28] and long-cavity lasers near the lasing threshold [16]. On the other hand, the dispersion in the fiber delay line can be quite strong in a long cavity laser and it can affect its dynamics very strongly. It was recently shown [22] that the evolution of the optical field in a linear fiber delay line can be described using a distributed term

$$B(t) = A(t) + P(t), \quad P(t) = -\sigma\int_0^\infty \frac{J_1(2\sqrt{\sigma s})}{\sqrt{\sigma s}}e^{-(\Gamma - i\Omega)s}A(t-s)ds,$$

where J_1 is the Bessel function, Γ and Ω represent full width at half maximum and central frequency of a Lorentzian absorption line, and σ represents total dispersion strength, which is proportional to the depth of Lorentzian absorption line and to the length of the fiber delay line L.

This time delay system was simulated numerically to demonstrate dynamics qualitatively similar to the experimentally observed output of various frequency-swept lasers, including static and quasistatic regimes [14, 16, 22, 28]. Moreover, it was shown that the most important dynamical features of the

FDML laser can be explained using linear stability analysis of the CW regimes of a static laser (lasing modes) [14, 22]. In particular, in the FDML regime, the laser produces chaotic output in one sweep direction and regular output with jumps between CW states with different frequencies that are closer to the frequency of the filter in another sweep direction (see Fig. 4 (b-1) and (b-4)), where the jumps correspond to a short wavelength modulational instability (MI) and chaotic output - to a long wavelength MI of lasing modes on the sides of the emission spectrum [14]. Finally, in the anomalous dispersion regime of the fiber delay line, all or some of the CW states can become unstable with respect to a long wavelength MI, thus impacting the quality of the output of a FDML laser [22].

This effect can be accurately captured by a more simple relation for the evolution of the field in the fiber, which can be obtained using the Padé approximant of the Lorentzian kernel [19]

$$B(t) = \left[-\frac{\sigma + 2i\Omega}{\sigma - 2i\Omega} A(t) + P(t) \right], \tag{3}$$

$$\frac{dP}{dt} = i\tilde{w}P - 2\frac{\Omega^2}{\sigma - 2i\Omega}P - \frac{4\sigma\Omega^2 A}{(\sigma - 2i\Omega)^2}. \tag{4}$$

We note that here we set $\Gamma = 0$ because polarisation $P(t)$ decays due to Landau damping, which appears due to Padé approximant. In the distributed case this effect is absent and Γ must be greater than zero. Since the approximation is valid for frequencies near 0, polarisation frequency is also shifted by $\tilde{w} \approx w$ to allow for near-constant dispersion strength inside the sweeping interval.

3.2 Modulational instability

In this section we analyse the stability of the lasing modes of a long-cavity laser, which helps us to understand its undesirable properties such as turbulent output. For that we substitute the CW solution $A(t) = A_0 e^{i\nu t}$, $G(t) = G_0$, $P(t) = P_0 e^{i\nu t}$ into the DDE system (1)-(4) to obtain

$$P_0 = \frac{4i\sigma\Omega^2 A_0}{(\sigma - 2i\Omega)\left(2i\Omega^2 - (\nu - \tilde{w})(\sigma - 2i\Omega)\right)},$$

$$B(t) = B_0 = A_0 e^{i\nu t} \frac{-i(\nu - \tilde{w})\sigma + 2(\nu - \tilde{w})\Omega + 2\Omega^2}{i(\nu - \tilde{w})\sigma + 2(\nu - \tilde{w})\Omega + 2\Omega^2},$$

$$G_0 = 2\log\frac{\gamma^2 + (w - \nu)^2}{\gamma^2\kappa},$$

$$A_0 = \sqrt{\frac{g_0 - G_0}{e^{G_0} - 1}}.$$

Here, $|B_0| = |A_0|$ and for $\nu \neq \tilde{w}$ the CW field exhibits an additional phase shift after going through fiber delay line. Since our approximation requires $|\nu - \tilde{w}| \ll |\Omega|$, this shift is small and can be neglected, thus we assume $\nu = \tilde{w}$ from now on.

Next, we linearise the system (1)-(4) near the CW state $A = (A_0 + \delta A e^{\lambda t})e^{i\nu t}$, $G = G_0 + \delta G e^{\lambda t}$, and $P = (P_0 + \delta P e^{\lambda t})e^{i\nu t}$ to obtain the following characteristic equation for the eigenvalues λ describing the stability of the CW solution:

$$a_2(\lambda)Y^2 + a_1(\lambda)Y + a_0(\lambda) = 0, \tag{5}$$

where

$$a_2(\lambda) = -\left(\left(\lambda^2\sigma^2 + 4\lambda\Omega^2(\lambda-\sigma) + 4\Omega^4\right)\left(\gamma^2 + (w-\nu)^2\right)\left(\left(A_0^2+1\right)\gamma_{g0} + \lambda\right)\right),$$
$$a_0(\lambda) = -\left(\left(\lambda^2\sigma^2 + 4\lambda\Omega^2(\lambda+\sigma) + 4\Omega^4\right)\left((\gamma+\lambda)^2 + (w-\nu)^2\right)\left(\left(A_0^2 e^{G_0}+1\right)\gamma_{g0} + \lambda\right)\right),$$
$$a_1(\lambda) = 2\lambda\Bigg(\gamma(\gamma+\lambda)\left(4\Omega^4 - \lambda^2\left(\sigma^2 - 4\Omega^2\right)\right) - 4\lambda^3\sigma\Omega(w-\nu) +$$
$$(w-\nu)^2\left(4\Omega^4 - \lambda^2\left(\sigma^2 - 4\Omega^2\right)\right)\Bigg) + \gamma_{g0}\Bigg(\gamma^2\big[4\Omega^4\left(A_0^2\left(e^{G_0}+1\right)+2\right) +$$
$$\lambda^2\left(4\alpha A_0^2\left(e^{G_0}-1\right)\sigma\Omega + \sigma^2\left(A_0^2\left(-\left(e^{G_0}+1\right)\right)-2\right) + 4\Omega^2\left(A_0^2\left(e^{G_0}+1\right)+2\right)\right)\big] +$$
$$\gamma\lambda\big[\lambda^2\left(4\alpha A_0^2\left(e^{G_0}-1\right)\sigma\Omega + \sigma^2\left(A_0^2\left(-\left(e^{G_0}+1\right)\right)-2\right) + 4\Omega^2\left(A_0^2\left(e^{G_0}+1\right)+2\right)\right) +$$
$$4\Omega^4\left(A_0^2\left(e^{G_0}+1\right)+2\right)\big] - (w-\nu)\big[8\lambda^3\sigma\Omega + 2\lambda^2\sigma^2(w-\nu) - 8\lambda^2\Omega^2(w-\nu) -$$
$$8\Omega^4(w-\nu) + A_0^2\big(\alpha\left(e^{G_0}-1\right)\lambda\left(\lambda^2\left(\sigma^2-4\Omega^2\right) - 4\lambda\sigma\Omega(w-\nu) - 4\Omega^4\right) +$$
$$\left(e^{G_0}+1\right)\left(4\lambda^3\sigma\Omega + \lambda^2\left(\sigma^2-4\Omega^2\right)(w-\nu) - 4\Omega^4(w-\nu)\right)\big)\big]\Bigg).$$

In the limit of large delay time $T \to \infty$ the eigenvalues belonging to the pseudo-continuous spectrum can be represented in the form $\lambda = i\mu + \frac{\Lambda}{T} + \mathcal{O}(1/T^2)$ with real μ [42]. Keeping only the single leading term $i\mu$ in $a_0(\lambda)$, $a_1(\lambda)$, $a_2(\lambda)$ and two leading terms $i\mu + \frac{\Lambda}{T}$ in $Y(\lambda)$, we obtain from (5) two branches of pseudo-continuous spectrum given by

$$\Lambda_\pm(\mu) + i\mu T = -\ln Y = -\ln\left[\frac{-a_1(i\mu) \pm \sqrt{a_1(i\mu)^2 - 4a_2(i\mu)a_0(i\mu)}}{2a_2(i\mu)}\right]. \tag{6}$$

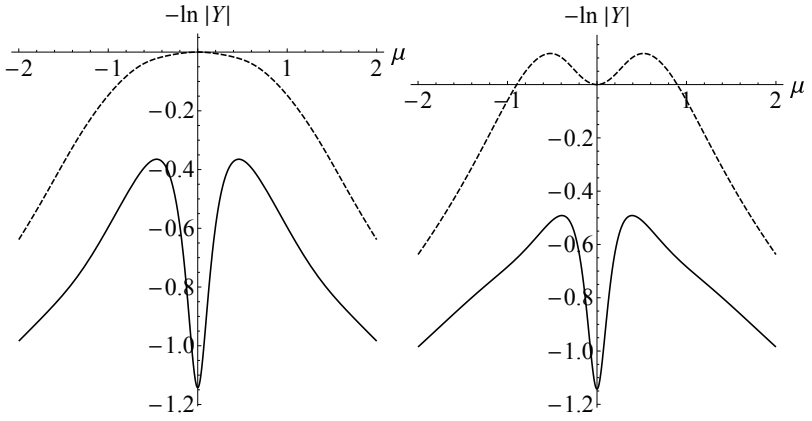

Figure 5: Real parts of two branches of the pseudo-continuous spectrum $\mathrm{Re}\Lambda_\pm(\mu)$ for the CW solutions (relative steady states) of (1)-(4) with $\kappa = 0.2$, $\gamma_g = 0.1$, $g_0 = 2$, $\nu = w = \tilde{w} = \varphi = 0$, $\Omega = -2$ obtained using equation (5), for the case of weak dispersion $\sigma = 1$ (left) and strong anomalous dispersion $\sigma = 4$ (right), where CW solution lost stability via a MI.

Due to the phase shift symmetry of Eqs. (1)-(4) one of the two eigenvalue branches $\Lambda_\pm(\mu)$ satisfies the condition $\Lambda(0) = 0$ (and $Y(0) = 1$). Long wavelength MI takes place when the second derivative of this branch $d^2\,\mathrm{Re}\,\Lambda(\mu)/d\mu^2$changes its sign at the point $\mu = 0$ from negative to positive, see Fig. 5. From $d^2\,\mathrm{Re}\,\Lambda(\mu)/d\mu^2 = \mathrm{Re}\left[\frac{Y''(0)}{Y(0)} - \frac{Y'(0)^2}{Y(0)^2}\right]$ and

$$Y'(0) = \frac{\sigma}{\Omega^2} + \frac{\gamma + \alpha(\nu - w)}{\gamma^2 + (w-\nu)^2}$$

we obtain the following condition for the MI of the CW state

$$-\frac{2\alpha\sigma}{\Omega^3}-\frac{(\gamma-\alpha(w-\nu))^2-\frac{2\left(\alpha^2+1\right)\left(\mathsf{A0}^2e^{\mathsf{G0}}+1\right)(w-\nu)^2}{\mathsf{A0}^2(e^{\mathsf{G0}}-1)}}{\left(\gamma^2+(w-\nu)^2\right)^2}\geq 0. \tag{7}$$

One can see that for zero dispersion $\sigma = 0$ the maximum gain mode $\nu = w$ is always stable. Modulational instability of the side modes can lead to bistability between chaotic state and CW states and, therefore, to the turbulent output of the laser during sweeping in case of normal dispersion [14].

Therefore, by choosing maximum gain mode $\nu = w$, we can obtain necessary condition for the MI of all the CW states in the anomalous dispersion regime $\Omega < 0$ [22]

$$\alpha D_2 L \leq -\frac{1}{\gamma^2}, \tag{8}$$

where $D_2 = \frac{2\sigma}{L\Omega^3} < 0$ corresponds to the second-order dispersion coefficient per unit length (L). By examining experimentally observed relations (see Fig. 2 (f), (e)), we can observe that with increasing wavelength the second-order dispersion coefficient $D_2 < 0$ increases by the absolute value, while parameters α and γ do not change significantly, hence the instability can be observed for smaller fiber length L in full agreement with condition (8) [22]. Moreover, this inequality coincides with the necessary condition in the case of distributed delay [22], which suggests that the approximate DDE system (1)-(4) is suitable for the investigation of the effect of the anomalous dispersion on the dynamics of long cavity lasers.

3.3 Numerical simulations

First, we assume $w = \tilde{w} = \Delta(t) = \delta \sin \rho t$ and note that by substituting a transformation

$$X(t) = \hat{X}(t)e^{i\int_{t-T}^{t}\Delta(\tau)d\tau}$$

for $X(t) = A(t), B(t)$, and $P(t)$ into equations (1), (3) one obtains the same equations for $\hat{X}(t) = \hat{A}(t), \hat{B}(t)$, and $\hat{P}(t)$ with the parameters $\hat{w} = 0$ and $\hat{\varphi} = -\int_{t-T}^{t}\Delta(\tau)d\tau$ [14]. In the case of fully synchronous FDML regime the filter is swept with a period exactly equal to the cavity round-trip time, i.e. $\rho = 2\pi/T$, and $\hat{\varphi} \equiv 0$, hence this case is completely equivalent to the static regime of operation. Moreover, the most practically relevant regime of operation with the period close to the cavity round trip time ($|\rho - 2\pi/T| \ll 1/T$) is formally equivalent to the quasistatic regime $|\rho| \ll 1/T$, because in both cases $\hat{\varphi}$ is a slowly varying function of time $d\hat{\varphi}/dt \ll 1/T$ [14].

Therefore, we perform numerical simulations only for the quasistatic regime of a frequency-swept FDML laser using the following parameters normalised to filter width ($\gamma = 1$): $T = 200$, $\kappa = 0.2$, $\delta = 5$, $\rho = 10^{-6}$, $\varphi = 0$, $\alpha = 2$, $\epsilon = 0.001$, $\gamma_g = 0.1$, $g_0 = 3$, $\Omega = -2$. For these parameters the laser operates in anomalous dispersion regime for $\sigma > 0$, and the MI of CW regimes can be observed according to (8) for

$$\sigma \geq 2.$$

We investigate numerically the effect of anomalous dispersion on the dynamics of the frequency-swept FDML laser. Similarly to experimental results depicted on Fig. 3, we can observe on Fig. 6 for zero dispersion strength $\sigma = 0$ the asymmetry of the output with respect to the sweep direction, where the output is chaotic before $\Delta(t)$ changes its sign, and after that it consists of more regular jumps between different CW regimes selected by the frequency-swept filter [14]. At the MI threshold $\sigma = 2$

we can see the same picture but the quality of the regular output degrades, and it further degrades for higher $\sigma = 2.2$ and $\sigma = 2.3$. We can still observe the change of sweep direction but no jumps, and for higher σ only turbulent output can be obtained. Therefore, we conclude that MI condition (8) can help us to determine if the FDML laser can produce regular output in the anomalous dispersion regime.

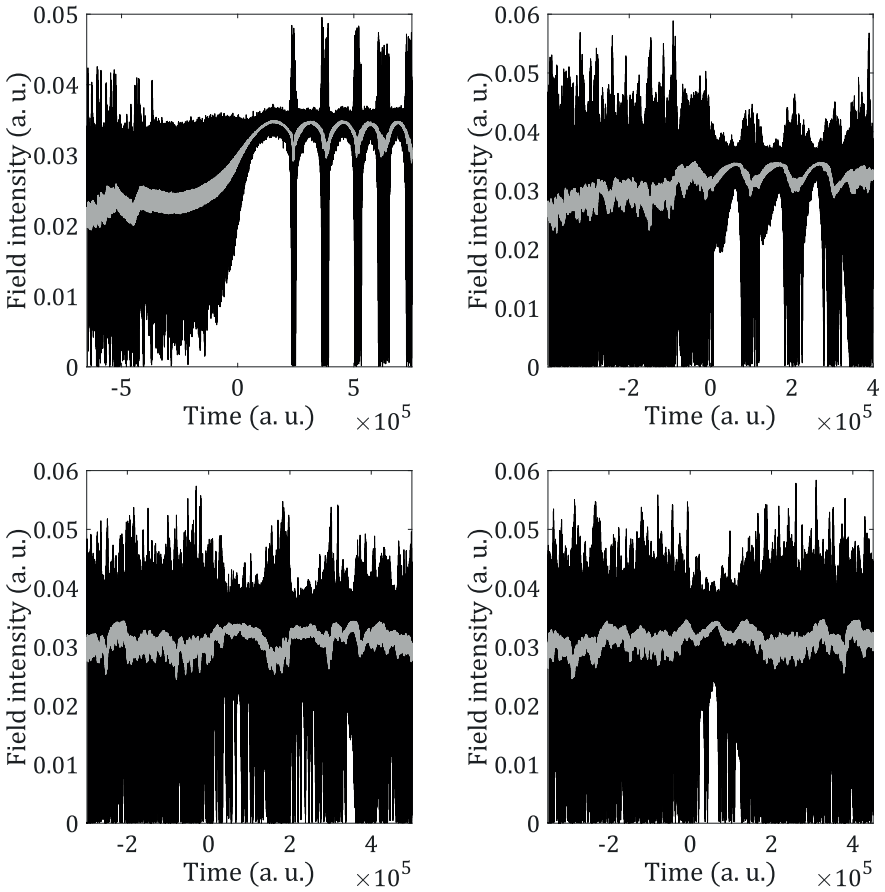

Figure 6: Numerical simulation of equations (1)-(3) in the quasistatic regime for different values of dispersion strength $\sigma = 0$ (top-left inset), $\sigma = 2$ (top-right), $\sigma = 2.2$ (bottom-left), $\sigma = 2.3$ (bottom-right). Other parameters are $\gamma = 1, T = 200, \kappa = 0.2, \delta = 5, \rho = 10^{-6}, \varphi = 0, \alpha = 2, \epsilon = 0.001$, $\gamma_g = 0.1$, $g_0 = 3, \Omega = -2$.

4 Conclusions

Long cavity semiconductor swept source lasers are important devices for many applications, however, they demonstrate different instabilities which affect their performance. In particular they can operate in a stable regime, turbulent regime or combination of the both, or emit stable localised structures which deteriorate their coherence. The laser cavity includes a long fiber delay which on one side is essential to ensure synchronisation between the modulation period and the cavity roundtrip time required for efficient lasing, but on the other side introduces chromatic dispersion which leads to desynchronisaton and is responsible for the variety of possible dynamical regimes. We study these regimes experimentally by using various experimental techniques such as optical heterodyne or a more recent real time electric field reconstruction technique developed to characterise lasers with sweeping frequency [32].

We demonstrate that stable and turbulent regimes can co-exist in such laser and investigate the stability conditions theoretically. The transition to turbulence can also be observed in other types of lasers and other systems such as hydrodynamical [23]. Theoretically, we propose a model of a long cavity semiconductor laser where a DDE for the optical field is coupled to two ordinary differential equations for carrier densities of an SOA and polarisation of the fiber delay line to account for chromatic dispersion. This model can successfully describe variety of dynamical regimes in the output of a swept source [14, 16, 28] discussed in this paper. We performed linear stability analysis of lasing modes to demonstrate that strong anomalous dispersion can lead to modulational instability of all the lasing modes and turbulent output of an FDML laser. We have derived analytically the necessary condition for the MI in this case, identified the instability threshold in the experiment [22], and demonstrated gradual degradation of the FDML regime for stronger anomalous dispersion experimentally and numerically under influence of noise. Main results of our study are the detailed description of dynamical regimes in a long cavity semiconductor swept source laser under different parameters and formalisation of stability criteria, which are important to overcome performance limitation of such lasers. Using our theoretical framework of delay differential equations, we have demonstrated analytically and numerically and confirmed experimentally, that the key dynamical features of long cavity fiber-based semiconductor lasers can be attributed to the basic nonlinear effects in the components of the device and their interaction in the cavity. In particular, multistability between CW and chaotic regimes in a laser with a static filter is due to long cavity and the SOA nonlinearity. In the quasistatic and the FDML regime, jumps between multiple CW states are related the destabilisation of the side modes under the modulated filter with respect to a short wavelength MI, whereas transition to the turbulent output is associated with a long wavelength MI, which could be potentially suppressed using an optical amplifier with very low linewidth enhancement factor [14]. Strong anomalous dispersion of the fiber can result in the destabilisation of all the lasing modes due to another long wavelength MI, hence dispersion compensation mechanisms should be applied to obtain coherent emission at corresponding wavelengths. In addition, these results can be further extended to other systems with time delay.

References

[1] Huang D, Swanson E A, Lin C P, Schuman J S, Stinson W G, Chang W, Hee M R, Flotte T, Gregory K, Puliafito C A et al. 1991 science **254** 1178–1181

[2] Chinn S, Swanson E and Fujimoto J 1997 Optics letters **22** 340–342

[3] Jiang Y, Karpf S and Jalali B 2020 Nature Photonics **14** 14–18

[4] Wieser W, Biedermann B R, Klein T, Eigenwillig C M and Huber R 2010 Optics express **18** 14685–14704

[5] John D D, Burgner C B, Potsaid B, Robertson M E, Lee B K, Choi W J, Cable A E, Fujimoto J G and Jayaraman V 2015 Journal of Lightwave Technology **33** 3461–3468

[6] Klein T and Huber R 2017 Biomedical optics express **8** 828–859

[7] Johnson B, Atia W, Kuznetsov M, Goldberg B D, Whitney P and Flanders D C 2017 Biomedical optics express **8** 1045–1055

[8] Eigenwillig C M, Wieser W, Todor S, Biedermann B R, Klein T, Jirauschek C and Huber R 2013 Nature communications **4** 1–7

[9] Karpf S and Jalali B 2019 Optics Letters **44** 5913–5916

[10] Bonesi M, Minneman M, Ensher J, Zabihian B, Sattmann H, Boschert P, Hoover E, Leitgeb R, Crawford M and Drexler W 2014 Optics express **22** 2632–2655

[11] Huber R, Wojtkowski M and Fujimoto J 2006 Optics express **14** 3225–3237

[12] Adler D C, Wieser W, Trepanier F, Schmitt J M and Huber R A 2011 Optics express **19** 20930–20939

[13] Pfeiffer T, Petermann M, Draxinger W, Jirauschek C and Huber R 2018 Biomedical optics express **9** 4130–4148

[14] Slepneva S, Kelleher B, O'Shaughnessy B, Hegarty S, Vladimirov A and Huyet G 2013 Optics express **21** 19240–19251

[15] Slepneva S, O'Shaughnessy B, Vladimirov A G, Rica S, Viktorov E A and Huyet G 2019 Optics express **27** 16395–16404

[16] Gowda U, Roche A, Pimenov A, Vladimirov A G, Slepneva S, Viktorov E A and Huyet G 2020 Optics Letters **45** 4903–4906

[17] Schmidt M, Pfeiffer T, Grill C, Huber R and Jirauschek C 2020 OSA Continuum **3** 1589–1607

[18] Girard S L, Piché M, Chen H, Schinn G W, Oh W Y and Bouma B E 2011 IEEE Journal of Selected Topics in Quantum Electronics **17** 1513–1520

[19] Pimenov A, Amiranashvili S and Vladimirov A G 2020 Mathematical Modelling of Natural Phenomena **15** 47

[20] Jiang T, Yin K, Wang C, You J, Ouyang H, Miao R, Zhang C, Wei K, Li H, Chen H et al. 2020 Photonics Research **8** 78–90

[21] Song Y, Wang Z, Wang C, Panajotov K and Zhang H 2020 Advanced Photonics **2** 024001

[22] Pimenov A, Slepneva S, Huyet G and Vladimirov A G 2017 Phys. Rev. Lett. **118**(19) 193901

[23] Turitsyna E, Smirnov S, Sugavanam S, Tarasov N, Shu X, Babin S, Podivilov E, Churkin D, Falkovich G and Turitsyn S 2013 Nature Photonics **7** 783–786

[24] Duport F, Schneider B, Smerieri A, Haelterman M and Massar S 2012 Optics express **20** 22783–22795

[25] Brunner D, Soriano M C, Mirasso C R and Fischer I 2013 Nature communications **4** 1–7

[26] Lepri S, Trono C and Giacomelli G 2017 Physical review letters **118** 123901

[27] Jirauschek C, Biedermann B and Huber R 2009 Optics express **17** 24013–24019

[28] Slepneva S, O'Shaughnessy B, Kelleher B, Hegarty S, Vladimirov A, Lyu H C, Karnowski K, Wojtkowski M and Huyet G 2014 Optics express **22** 18177–18185

[29] Butler T P, Slepneva S, McNamara P, Neuhaus K, Goulding D, Leahy M and Huyet G 2017 IEEE Photonics Journal **9** 1–10

[30] Kane D J and Trebino R 1993 IEEE Journal of Quantum Electronics **29** 571–579

[31] Xin Y C, Kane D and Lester L 2008 Electronics Letters **44** 1255–1257

[32] Butler T, Slepneva S, O'Shaughnessy B, Kelleher B, Goulding D, Hegarty S, Lyu H C, Karnowski K, Wojtkowski M and Huyet G 2015 Optics letters **40** 2277–2280

[33] Butler T 2016 Real-time characterisation of dynamic laser fields Ph.D. thesis Cork Institute of Technology

[34] Choma M A, Yang C and Izatt J A 2003 Optics letters **28** 2162–2164

[35] Kelleher B, Goulding D, Pascual B B, Hegarty S P and Huyet G 2010 The European Physical Journal D **58** 175–179

[36] Huyet G, Porta P, Hegarty S, McInerney J and Holland F 2000 Optics communications **180** 339–344

[37] Aranson I S and Kramer L 2002 Reviews of modern physics **74** 99

[38] Nozaki K and Bekki N 1984 Journal of the Physical Society of Japan **53** 1581–1582

[39] Butler T P, Goulding D, Kelleher B, O'Shaughnessy B, Slepneva S, Hegarty S P and Huyet G 2017 Optics Express **25** 27464–27474

[40] Bilenca A, Yun S, Tearney G and Bouma B 2006 Optics letters **31** 760–762

[41] Kraetschmer T and Sanders S T 2009 Ultrastable fourier domain mode locking observed in a laser sweeping 1363.8–1367.3 nm 2009 Conference on Lasers and Electro-Optics and 2009 Conference on Quantum electronics and Laser Science Conference (IEEE) pp 1–2

[42] Yanchuk S and Wolfrum M 2010 SIAM J. Appl. Dyn. Syst. **9** 519–535